Tetrahedron Letters 54 (2013) 3353–3358

Contents lists available at SciVerse ScienceDirect

Tetrahedron Letters

journal homepage: www.elsevier.com/locate/tetlet

1,8-Naphthalimide-based 'turn-on' fluorescent sensor for the detection of zinc ion in aqueous media and its applications for bioimaging

Li Yun Zhao [a], Qi Li Mi [c,d], Guang Ke Wang [a], Jian Hua Chen [c], Jun Feng Zhang [b,*], Qi Hua Zhao [a,*], Ying Zhou [a,*]

[a] Key Laboratory of Medicinal Chemistry for Natural Resource, School of Chemical Science and Technology, Yunnan University, Kunming 650091, PR China
[b] College of Chemistry and Chemical Engineering, Yunnan Normal University, Kunming 650500, PR China
[c] Yunnan Academy of Tobacco Science, Kunming 650106, Yunnan Province, PR China
[d] Yunnan Institute of Microbiology, Yunnan University, Kunming 650091, PR China

ARTICLE INFO

Article history:
Received 23 January 2013
Revised 7 April 2013
Accepted 15 April 2013
Available online 20 April 2013

Keywords:
Fluorescence probe
Zinc ion
1,8-Naphthalimide
Imaging agents
Cytokinesis-block micronucleus

ABSTRACT

A 1,8-naphthalimide derivative (**1**) was intentionally designed and synthesized as a new turn-on fluorescent probe for the detection of zinc ion with high selectivity over other metal ions at pH 7.4 in aqueous media (CH_3CN/HEPES, V/V = 6:4). The reaction mechanism is attributed to the replacement of the protons of the O–H groups by zinc ion at the binding site and production of fluorescence which is blocked in the photo-induced electron transfer (PET) process. Remarkable enhancement of up to 13-fold in fluorescence intensity with a 38 nm red-shift was achieved in the detection of zinc ion. Compound **1** was successfully applied to the fluorescence imaging of zinc ion, with a fluorescence emission color produced in the cell nucleus different from that produced in the cytoplasm, in A549, BEAS-2B, CHO, Hela, and HepG2 cells. Furthermore, cytokinesis-block micronucleus (CBMN) assay was carried out in CHO cells using **1** and zinc ion as the imaging agents, showing that the **1**-Zn^{2+} agent is a nucleic acid selective stain, which could be applied in MN assays in different kinds of cell lines.

1. Introduction

Because of the high sensitivity, specificity, simplicity of implementation, and fast response time, fluorescent probes for detecting metal ions possess innate advantages over other detection methods developed, such as high performance liquid chromatography[1] and capillary electrophoresis.[2] Fluorescent probes also offer applications for both in vitro assays and in vivo imaging studies.[3] In particular, the development of a fluorescent probe for zinc ion in the presence of a variety of other metal ions has received considerable attention.[4,5] Zn^{2+} is involved in a variety of physiological and pathological processes, such as Alzheimer's disease, epilepsy, ischemic stroke, and infantile diarrhea.[6] It is also reported that zinc ion is a potent killer of neurons via oxidative stress.[7] A decrease in the concentration of Zn^{2+} can cause a reduction in the ability of the islet cells of the pancreas to produce and secrete insulin.[8] Accordingly, development of Zn^{2+} selective fluorescent sensors and convenient methods to detect intracellular Zn^{2+} ion are certainly important issues in recent years. The total concentration of Zn^{2+} in different cells varies from the nanomolar range up to about 0.3 mM,[9] which means that optimized chemical probes are required to monitor zinc concentration over that broad range.

Most of the fluorescence-based probes for Zn^{2+} suffer from limitations due to tight binding affinity or lack of sufficient selectivity to detect intrinsic levels of Zn^{2+} in pancreatic islets. Therefore, it remains a challenge to develop efficient fluorescent probes with high sensitivity and selectivity for the detection of metal ions in biological applications. Recently, a rhodamine-based derivative bearing a *N*-butyl-1,8-naphthalimide group was reported in our work, in which it displayed a selective colorimetric and fluorescence change toward Cu^{2+} based on the rhodamine ring-opening approach.[10] Meanwhile, some simple but efficient fluorescent sensors based on Shift base, which displayed selective optical responses, were reported.[11] In order to further explore the sensing mechanism of this series of 1,8-naphthalimide-based compounds and their biological applications, the introduction of new ligands with different binding points has attracted considerable interest.

Herein, we describe the synthesis and the photophysical properties of a new 1,8-naphthalimide-based chemosensor **1**, which has been designed for the sensitive and selective 'turn-on' fluorescence detection of Zn^{2+} in aqueous solvents (CH_3CN/HEPES, V/V = 6:4, 0.02 M HEPES buffer, pH 7.4) as well as in intracellular media. As expected, upon addition of 20 equiv of various metal ions, only Zn^{2+} leads to a significant enhancement of up to 13-fold in fluorescence intensity with a 38 nm red-shift, and no obvious

* Corresponding authors.
E-mail addresses: junfengzhang78@yahoo.cn (J. F. Zhang), qhzhao@ynu.edu.cn (Q. H. Zhao), yingzhou@ynu.edu.cn (Y. Zhou).

0040-4039/$ - see front matter Crown Copyright © 2013 Published by Elsevier Ltd. All rights reserved.
http://dx.doi.org/10.1016/j.tetlet.2013.04.045

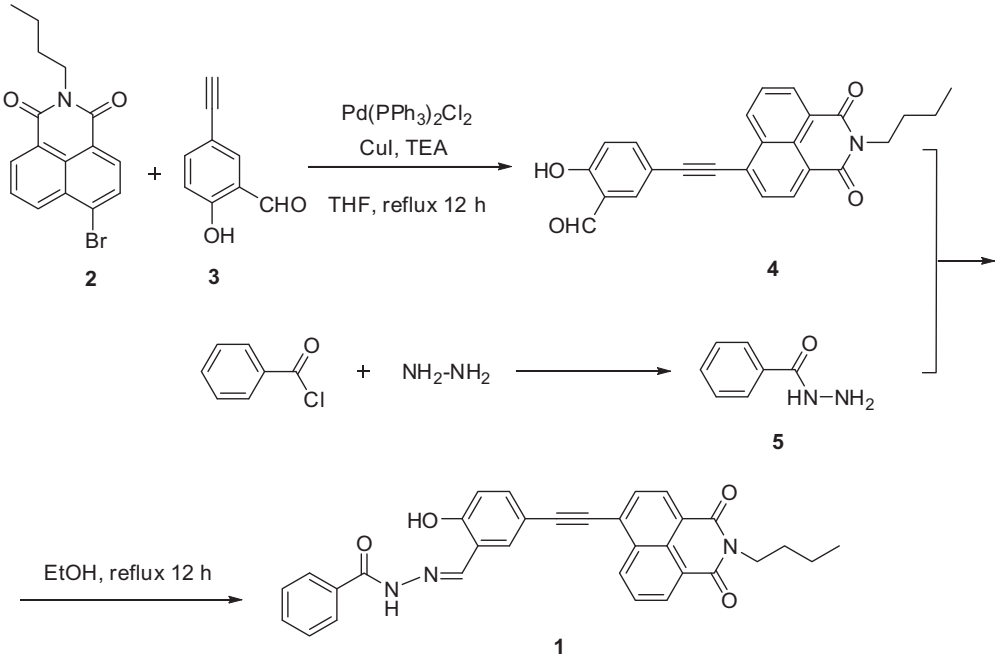

Scheme 1. The synthetic route of compound **1**.

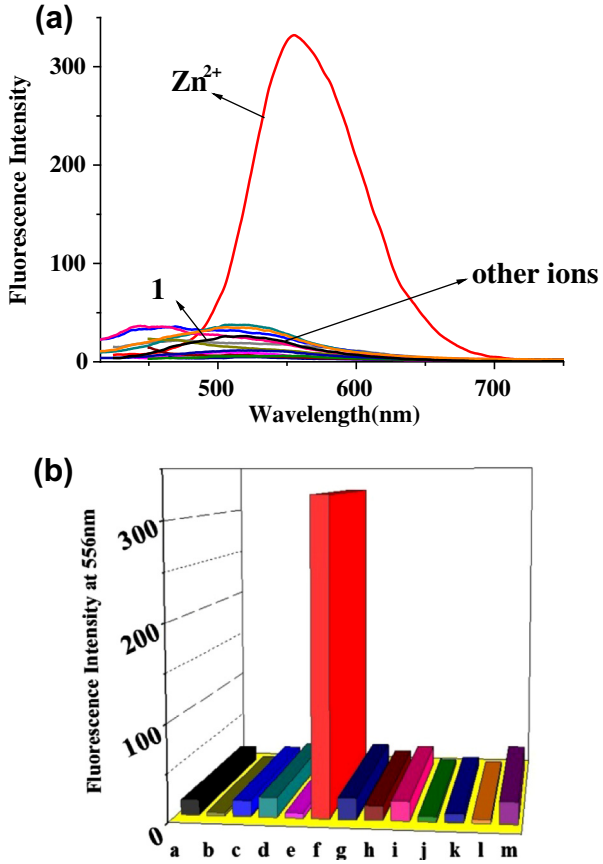

Figure 1. (a) Fluorescence emission spectra of **1** (2.0×10^{-5} M) in CH_3CN–HEPES buffer (0.02 M, pH 7.4) (V/V = 6:4) with 20 equiv of Na^+, Co^{2+}, Ni^{2+}, Cu^{2+}, Zn^{2+}, Pb^{2+}, Cd^{2+}, Ag^+, Hg^{2+}, Fe^{2+}, Mg^{2+}, and Cr^{3+}. (b) Fluorescence intensity of **1** (2.0×10^{-5} M) at 556 nm after addition of 20 equiv of selected ions in CH_3CN–HEPES buffer (0.02 M, pH 7.4) (V/V = 6:4) (a: **1**, b: Co^{2+}, c: Cd^{2+}, d: Hg^{2+}, e: Cu^{2+}, f: Zn^{2+}, g: Na^+, h: Ag^+, i: Pb^{2+}, j: Fe^{2+}, k: Mg^{2+}, l: Ni^{2+}, m: Cr^{3+}).

fluorescence change was observed for other tested metal ions. Furthermore, chemosensor **1** presents high sensitivity and selectivity in the fluorescence imaging of Zn^{2+} in A549, BEAS-2B, CHO, Hela, and HepG2 cells. With differing binding capacities toward different nucleic acids (DNA and RNA), not characteristic of most of other imaging agents, **1** exhibits a fluorescence emission color in the cell nucleus different from that in the cytoplasm. It provides a clear fluorescence image of the tested cells. Cytokinesis-block

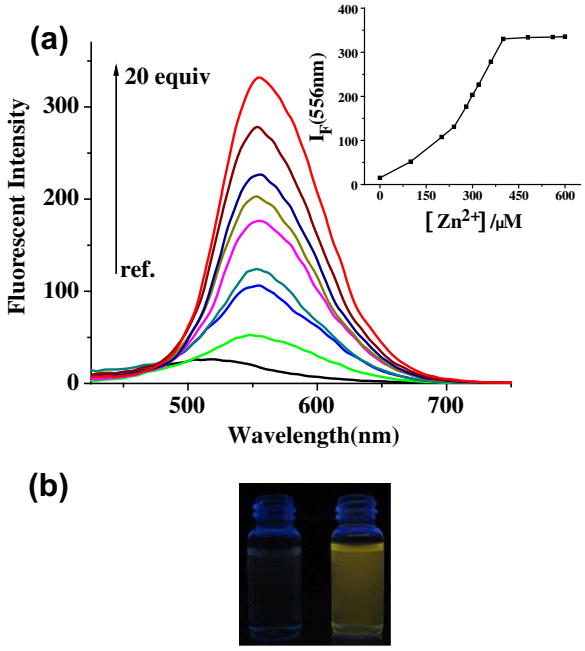

Figure 2. (a) Fluorescence emission titration spectra of **1** (2.0×10^{-5} M) in the presence of varying concentrations of Zn^{2+} in CH_3CN–HEPES buffer (0.02 M, pH 7.4) (V/V = 6:4). Excitation wavelength was 410 nm. Inset: fluorescence intensity of **1** (2.0×10^{-5} M) at 556 nm as a function of varying concentrations of Zn^{2+}. (b) Fluorescence picture of compound **1** (left) and compound **1** upon the addition of 20 equiv of Zn^{2+} (right).

micronucleus (CBMN) assay was also successfully carried out in CHO cells using **1** and zinc ion as the imaging agents. It showed that **1**-Zn^{2+} agent is a nucleic acid selective stain, which is useful for MN assays in different kinds of cell lines. The application of sensor **1** for detecting Zn^{2+} for in vitro assays and for in vivo imaging studies broadens the opportunities for designing new fluorescent chemodosimeters in the ion detection field.

2. Synthesis and photophysical properties of 1

As shown in Scheme 1 4-(5′-ethynylsalicylaldehyde)-*N*-butyl-1,8-naphthalimides (**4**) was synthesized according to our reported procedure with an improved yield of 83%.[10] Compound **5** was synthesized by modifying the literature method with a high yield of 90%.[12] Compound **4** was then reacted with **5** in ethanol to give the target compound **1** in 58% yield.[13] The detailed experimental procedures of the new compounds are described in Supplementary data.

3. Detection of Zn^{2+} ions

In order to clarify the interaction of **1** with metal ions, the UV–vis absorption and fluorescence spectra of **1** were studied in CH_3CN–HEPES buffer (0.02 M, pH 7.4) (V/V=6:4) solutions. Na^+, Co^{2+}, Ni^{2+}, Cu^{2+}, Zn^{2+}, Pb^{2+}, Cd^{2+}, Ag^+, Hg^{2+}, Fe^{2+}, Mg^{2+}, and Cr^{3+} were used to measure the selectivity of probe **1**, and fluorescence spectra were recorded after three minutes upon addition of 20 equiv of each of these ions. As shown in Fig. S1, in the absence of ions, the maximum absorption wavelength of **1** is at about 397 nm. Upon addition of different metal ions, obvious red shifts of the absorption maximum could be found in the presence of Zn^{2+}, Cd^{2+}, Cu^{2+}, Co^{2+}, Ni^{2+}, Fe^{2+}, and Pb^{2+}, bringing dramatic color changes from light yellow to saffron yellow. It revealed that **1** had no obvious selectivity in the absorption toward the tested ions. However, in the fluorescence tests, compared to other ions examined, only Zn^{2+} generated a significant "turn-on" fluorescence response at 556 nm with a 38 nm red-shift. The fluorescence of **1** was very weak (Φ = 0.016), and a fluorescence enhancement of up to 13-fold was found in the presence of Zn^{2+} (Fig. 1a). No significant fluorescence change was observed in the presence of other ions. As shown in Figure 1b, the obvious fluorescence enhancement, which is induced by Zn^{2+} is obvious to the naked eye.

To get further insight into the binding of Zn^{2+} with **1**, the fluorescence spectra of **1** upon titration with different equiv of Zn^{2+} were recorded. As shown in Figure 2, **1** exhibited a very weak fluorescence at 518 nm. Upon addition of increasing

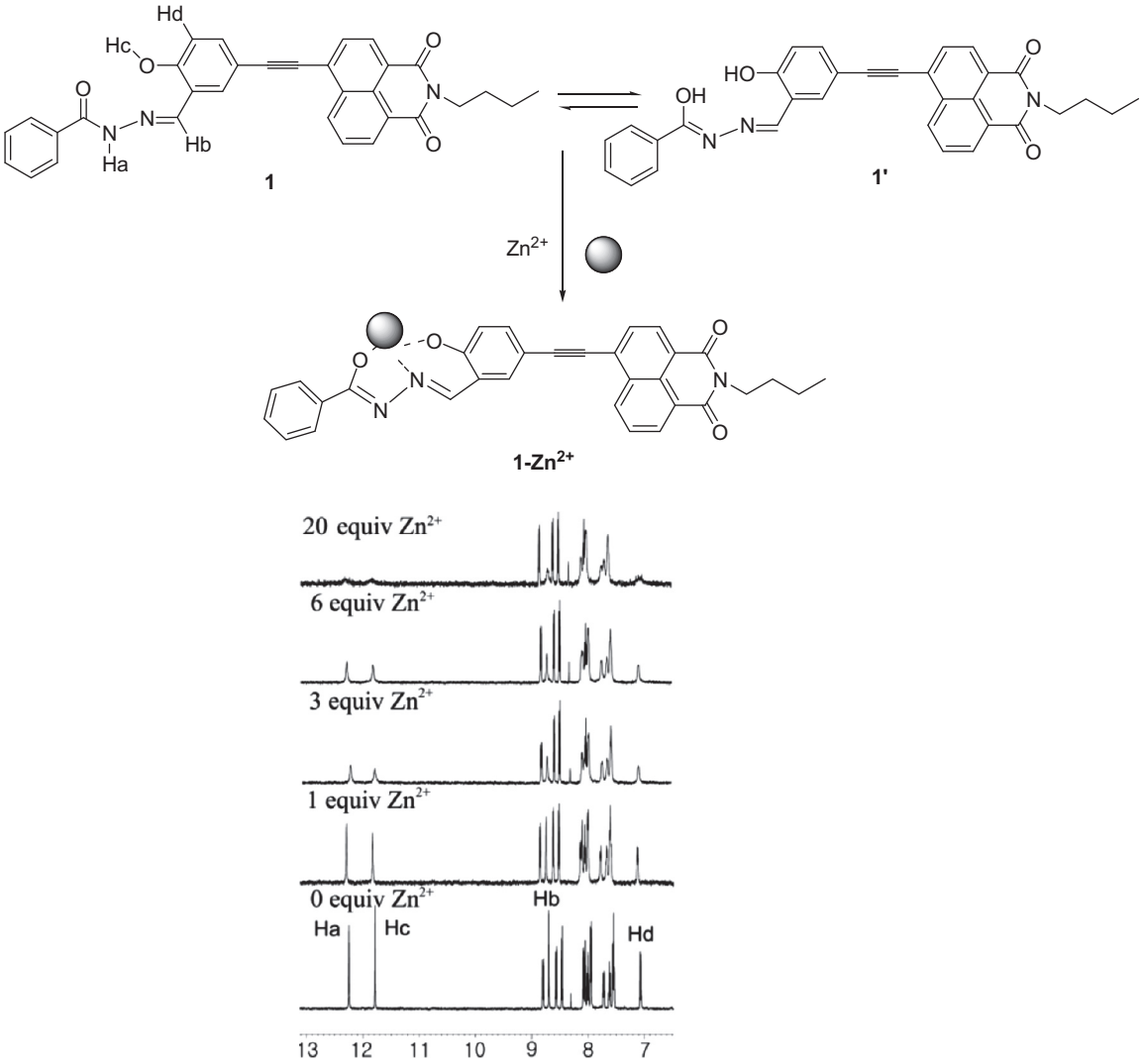

Figure 3. The proposed binding mechanism of compound **1** with Zn^{2+} and ^1H NMR spectra of compound **1** (0.5 mM) with Zn^{2+} in DMSO-d_6; equivalents of Zn^{2+} are related to the concentration of compound **1**.

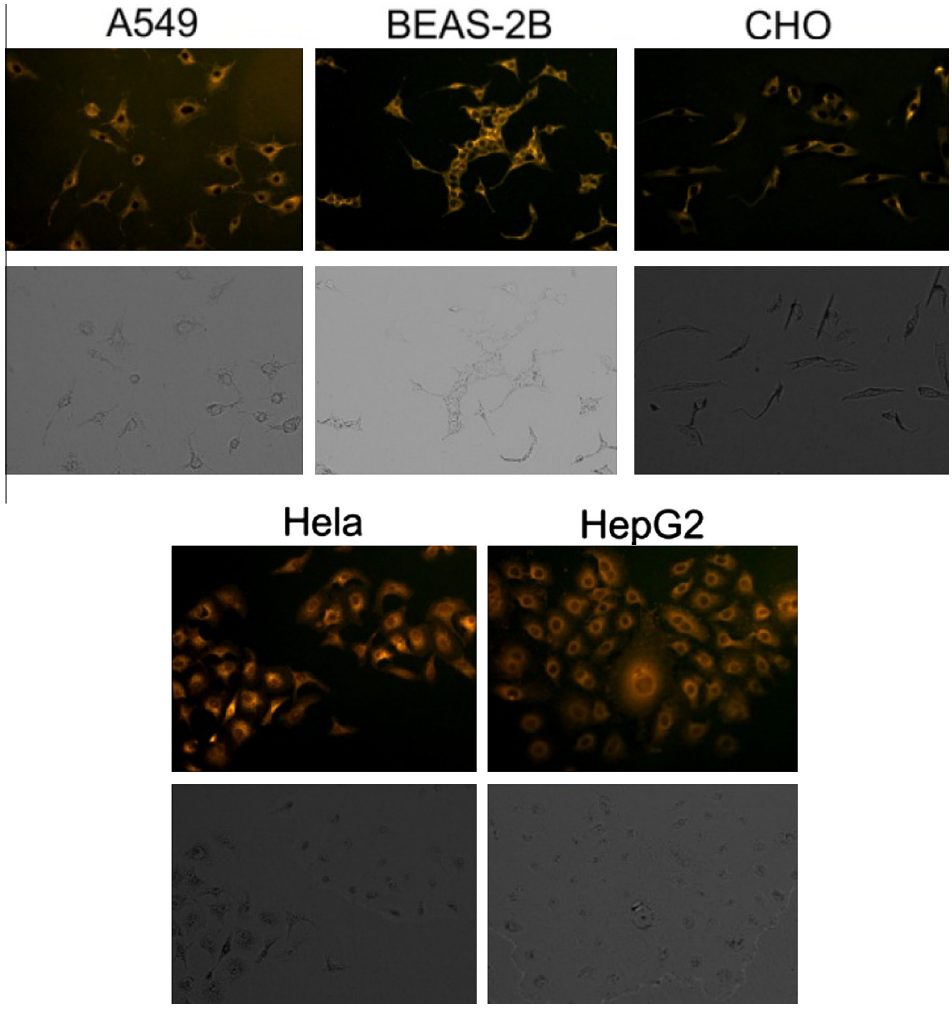

Figure 4. Confocal microscopy images of A549, BEAS-2B, CHO, Hela, and HepG2 cells treated with **1** (20 μM) and Zn^{2+} (400 μM). Cell images were obtained using B-2A Ex 450–490 (DM505, BA520) channel at a magnification of 200. The top panels are the fluorescence image of the corresponding tested cells. The bottom panels show the bright image of the corresponding tested cells.

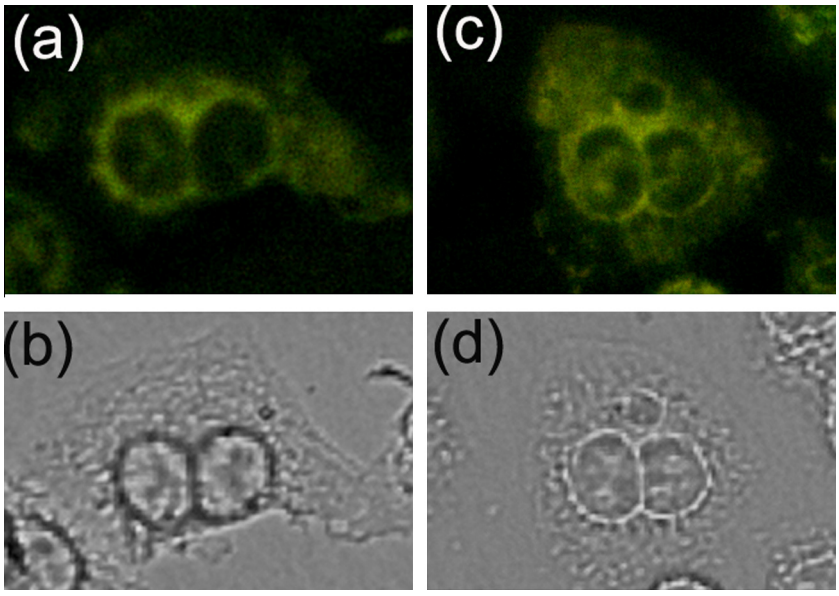

Figure 5. (a) Fluorescence microscopy images of representative binucleated (BN) CHO cell, **1** (20 μM) and Zn^{2+} (400 μM) as imaging agent. (b) Bright fields of the BN CHO cell. (c) Fluorescence microscopy images of representative binucleated (BN) cells with micronuclei (MN) using **1** (20 μM) and Zn^{2+} (400 μM) as imaging agent. (d) Bright fields of BN cells with micronuclei (MN). Cell images were obtained using B-2A Ex 450–490 (DM505, BA520) channels at a magnification of 200.

amounts of Zn^{2+}, the fluorescence band at 518 nm was gradually red-shifted and replaced by a new band at 556 nm. An obvious 13-fold enhancement was observed and saturated with 20 equiv of Zn^{2+} within 3 min. These results suggested that probe **1** displayed an excellent selectivity toward Zn^{2+} by fluorescence changes (Fig. 2).

To explore the possibility of using **1** as a Zn^{2+} selective fluorescent chemosensor, comparision experiments were carried out. **1** (20 μM) was first mixed with 20 equiv of Zn^{2+}, followed by adding 30 equiv of various metal ions including Na^+, Co^{2+}, Ni^{2+}, Cu^{2+}, Pb^{2+}, Cd^{2+}, Ag^+, Hg^{2+}, Fe^{2+}, Mg^{2+}, and Cr^{3+}. The comparison event was monitored by the fluorescence emission changes. In the presence of Co^{2+}, Cu^{2+}, Fe^{2+}, and Ag^+, the fluorescence intensity at 556 nm decreased little (Fig. S3), while in the presence of Na^+, Ni^{2+}, Pb^{2+}, Cd^{2+}, Hg^{2+}, Mg^{2+}, and Cr^{3+}, the emission spectra were almost identical to which was obtained in the presence of Zn^{2+} alone. Therefore, **1** was proved to be a promising selective fluorescent detector for Zn^{2+} in the presence of most competing metal ions.

The linear dependence of the intensity ratio within the equivalent range of Zn^{2+} ion showed that **1** forms a 1:1 complex with Zn^{2+}, whose association constant (K_a) was determined to be about $3.02 \times 10^3\ M^{-1}$ from the titration experiments.[14] Moreover, Job's plot (Fig. S4) confirmed 1:1 stoichiometry for the **1**–Zn(II) complex, which strongly supported the above conclusions. Mass–spectrometry analysis of a product obtained from the reaction of **1** with $Zn(ClO_4)_2$ in $CHCl_3$ also supported the formation of a **1**-Zn^{2+} adduct (Fig. S5). A peak at 578.34 corresponding to $[\mathbf{1}+Zn]^{2+}$ was clearly observed. To investigate the detection limit of **1** for Zn^{2+}, **1** (0.2 μM) was treated with various concentrations of Zn^{2+} (0–4 μM). The fluorescence intensity at 556 nm was plotted as a function of the Zn^{2+} concentration. The fluorescence intensity of **1** is linearly proportional to Zn^{2+} concentrations of 0–4 μM, and detection limit as low as 1.03×10^{-6} M concentration of Zn^{2+} was established by using **1** with a signal-to-noise ratio of 3.

Further NMR spectroscopic analysis also provided evidence for the replacement of protons at the binding sites in **1** (Fig. 3). With addition of varying concentrations of $Zn(ClO_4)_2$ to **1** (0.5 mM) in DMSO-*d6*, the peaks of Ha and Hc in the binding sites decreased with increasing concentration of $Zn(ClO_4)_2$ and eventually disappeared. Simultaneously, the other two peaks of Hb and Hd decreased sharply. All the results showed that the replacement of protons resulted from the binding of Zn^{2+} and confirmed the formation of a cation–receptor complex.

4. Biological applications

To test the capability of **1**-Zn^{2+} for imaging cells, five ethanol-fixed cell lines (A549, BEAS-2B, CHO, Hela, and HepG2 cells) were imaged using **1**-Zn^{2+} as the imaging agent. As shown in Figure 4, different fluorescence emission colors were observed in the cell nucleus and in the cytoplasm. The cells exhibited deep-purple fluorescence in the nuclei and bright-yellow fluorescence in the cytoplasm, providing a clear fluorescence image of the tested cells, and indicating that the **1**-Zn^{2+} agent showed different binding capacities toward different nucleic acids (DNA and RNA) in the cells tested (Fig. 4).

To detect whether the **1**-Zn^{2+} agent could be used in micronucleus assay as imaging agent, cytokinesis-block micronucleus (CBMN) assay was carried out in CHO cells using colchicine (0.5 μg/ml) as micronuclei induced reagent (Fig. 5). Differential staining of nuclear material and cytoplasm was also observed clearly and easily, using the **1**-Zn^{2+} agent as fluorescent dye. Deduced from the above results, **1**-Zn^{2+} agent is a nucleic acid selective stain, which could be applied in MN assays in different kinds of cell lines.

5. Conclusions

This study examined the binding properties of a new 1,8-naphthalimide derivative (**1**) for various cations, and the results showed that **1** is a new turn-on fluorescent probe for the detection of zinc ion with high selectivity over other metal ions at pH 7.4 in aqueous media (CH_3CN/HEPES, V/V = 6:4). Remarkable enhancement of up to 13-fold in fluorescence intensity with a 38 nm red-shift was only observed in the presence of Zn^{2+}. Compound **1** was successfully applied to the fluorescence imaging of zinc ion in different cells and cytokinesis-block micronucleus (CBMN) assay. In A549, BEAS-2B, CHO, Hela, and HepG2 cells, **1**-Zn^{2+} agent exhibited different fluorescence emission colors in the cell nucleus and in the cytoplasm. A similar phenomenon was also observed in the staining of nuclear material and cytoplasm using the **1**-Zn^{2+} agent as fluorescent dye in CBMN assay carried out in CHO cells, showing that **1**-Zn^{2+} agent was a nucleic acid selective stain, which could be applied in MN assays in different kinds of cell lines.

Acknowledgments

This work was supported by the Natural Science Foundation of China (NSFC Grant Nos. 21061016, 21102127, 21262045 and 21262050); the Foundation of the Department of Science and Technology of Yunnan Province of China (Nos. 2011FB013 and 2011FB047); the Open Fund of Key Laboratory of Medicinal Chemistry for Natural Resource (No. 2011122002).

Supplementary data

Supplementary data associated with this article can be found, in the online version, at http://dx.doi.org/10.1016/j.tetlet.2013.04.045.

References and notes

1. (a) Chwatko, G.; Bald, E. *Talanta* **2000**, *52*, 509–515; (b) Nolin, T. D.; McMenamin, M. E.; Himmelfarb, J. *J. Chromatogr., B: Anal. Technol. Biomed. Life Sci.* **2007**, *852*, 554–561.
2. (a) Ivanov, A. R.; Nazimov, I. V.; Baratova, L. A. *J. Chromatogr. A* **2000**, *870*, 433–442; (b) Amarnath, K.; Amarnath, V.; Amarnath, K.; Valentine, H. L.; Valentine, W. M. *Talanta* **2003**, *60*, 1229–1238; (c) Chen, G.; Zhang, L.; Wang, J. *Talanta* **2004**, *64*, 1018–1023.
3. (a) Chen, X. Q.; Zhou, Y.; Peng, X. J.; Yoon, J. *Chem. Soc. Rev.* **2010**, *39*, 2120–2135; (b) Zhou, Y.; Xu, Z. C.; Yoon, J. *Chem. Soc. Rev.* **2011**, *40*, 2222–2235; (c) Zhou, Y.; Yoon, J. *Chem. Soc. Rev.* **2012**, *41*, 52–67; (d) Zhang, J. F.; Zhou, Y.; Yoon, J.; Kim, J. S. *Chem. Soc. Rev.* **2011**, *40*, 3416–3429; (e) Kim, H. N.; Ren, W. X.; Kim, J. S.; Yoon, J. *Chem. Soc. Rev.* **2012**, *41*, 3210–3244; (f) Chen, X.; Pradhan, T.; Wang, F.; Kim, J. S.; Yoon, J. *Chem. Rev.* **2012**, *112*, 1910–1956.
4. (a) Jiang, P.; Guo, J. *Coord. Chem. Rev.* **2004**, *248*, 205–229; (b) Que, E. L.; Domaille, D. W.; Chang, C. J. *Chem. Rev.* **2008**, *108*, 1517–1549; (c) Xu, Z. C.; Yoon, J.; Spring, D. R. *Chem. Soc. Rev.* **2010**, *39*, 1996–2006.
5. (a) Manandhar, E.; Broome, J. H.; Myrick, J.; Lagrone, W.; Cragg, P. J. *Chem. Commun.* **2011**, 8796–8798; (b) Chen, M. L.; Lv, X.; Liu, Y. L.; Zhao, Y.; Liu, J.; Wang, P.; Guo, W. *Org. Biomol. Chem.* **2011**, *9*, 2345–2349; (c) Bhalla, V.; Roopa, N.; Kumar, M. *Org. Lett.* **2012**, *14*, 2802–2805; (d) Li, M.; Lu, H. Y.; Liu, R. L.; Chen, J. D.; Chen, C. F. *J. Org. Chem.* **2012**, *77*, 3670–3673.
6. (a) Bush, A. I.; Pettingell, W. H.; Multhaup, G.; Paradis, M.; Vonsattel, J.-P.; Gusella, J. F.; Beyreuther, K.; Maeters, C. L.; Tanzi, R. E. *Science* **1994**, *265*, 1464–1467; (b) Koh, J. Y.; Suh, S. W.; Gwag, B. J.; He, Y. Y.; Hsu, C. Y.; Choi, D. W. *Science* **1996**, *271*, 1013; (c) Walker, C. F.; Black, R. E. *Annu. Rev. Nutr.* **2004**, *24*, 255–275.
7. Frederickson, C. J.; Koh, J. Y.; Bush, A. I. *Nat. Rev. Neurosci.* **2005**, *6*, 449–462.
8. Chausmer, A. B. *J. Am. Coll. Nutr.* **1998**, *17*, 109–115.
9. Quarterman, J.; Mills, C. F.; Humphries, W. R. *Biophys. Res. Commun.* **1966**, *25*, 354–358.
10. Zhang, J. F.; Zhou, Y.; Yoon, J.; Kim, Y.; Kim, S. J.; Kim, J. S. *Org. Lett.* **2010**, *12*, 3852–3855.
11. (a) Zhou, Y.; Wang, F.; Kim, Y.; Kim, S.; Yoon, J. *Org. Lett.* **2009**, *11*, 4442–4445; (b) Zhou, Y.; Kim, Y. Z.; Yoon, J. *Bioorg. Med. Chem. Lett.* **2010**, *20*, 125–128; (c) Zhou, Y.; Jung, J. Y.; Jeon, H. R.; Kim, Y.; Kim, S.; Yoon, J. *Org. Lett.* **2011**, *13*, 2742–2745; (d) Wang, L.; Qin, W.; Liu, W. *Inorg. Chem. Commun.* **2010**, *13*, 1122–1125; (e) Lin, H.; Cheng, P.; Wan, C.; Wu, A. *Analyst* **2012**, *137*, 4415–4417.

12. Isaad, J.; Perwuelz, A. *Tetrahedron Lett.* **2010**, *51*, 5328–5332.
13. ^{1}H NMR (500 MHz, DMSO-d_6) δ (ppm): 12.248 (s, 1H), 11.783 (s, 1H), 8.805–8.789 (d, 1H), 8.694 (s, 1H), 8.570–8.556 (d, 1H), 8.471–8.456 (d, 1H), 8.084–7.940 (m, 5H), 7.731–7.711 (d, 1H), 7.616–7.531 (m, 3H), 7.071–7.054 (d, 1H), 4.053–4.024 (m, 2H), 1.627–1.582 (m, 2H), 1.370–1.326 (m, 2H), 0.931–0.902 (m, 3H). ^{13}C NMR (100 MHz, $CDCl_3$) δ(ppm): 164.4, 164.1, 159.4, 149.5, 135.2, 134.6, 132.7, 132.4, 131.8, 131.6, 130.5, 128.7, 128.2, 127.7, 127.5, 122.9, 121.7, 118.6, 117.9, 113.2, 99.1, 85.3, 77.6, 77.3, 77.0, 40.4, 30.2, 20.4, 13.8. Mass calcd for $C_{32}H_{25}N_3O_4$ (m/z = 515.18), positive ESIMS m/z $[M+K]^+$ = 538.18; positive ESIMS m/z $[M+Na]^+$ = 554.18.
14. Association constants were obtained using the computer program Enzfitter, available from Elsevier-BIOSOFT, 68 Hills Road, Cambridge CB2 1LA, UK.